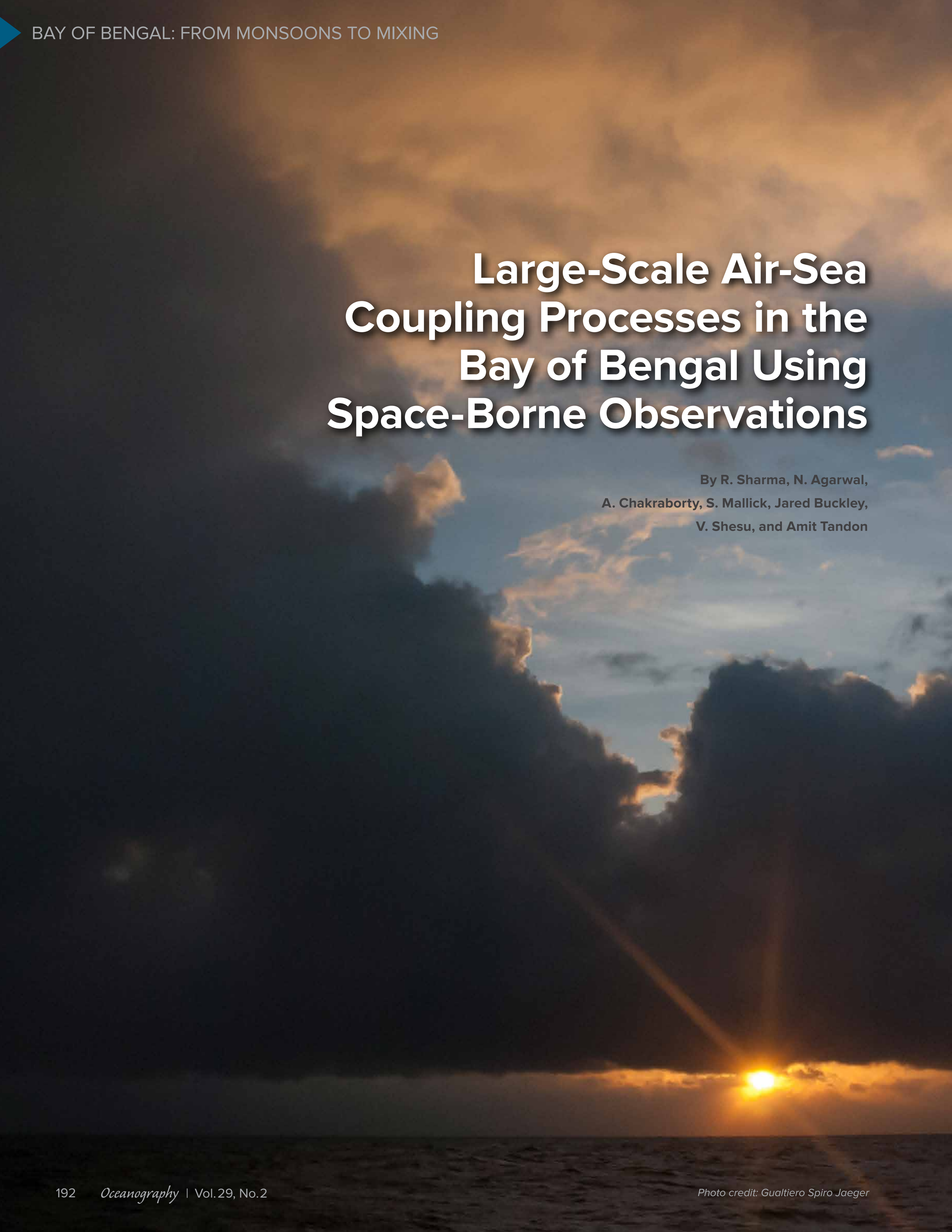

Large-Scale Air-Sea Coupling Processes in the Bay of Bengal Using Space-Borne Observations

By R. Sharma, N. Agarwal, A. Chakraborty, S. Mallick, Jared Buckley, V. Shesu, and Amit Tandon

Photo credit: Gualtiero Spiro Jaeger

ABSTRACT. For the last several decades, sensors aboard satellites have provided a rich array of information about ocean surface parameters, especially sea surface temperature. The latest addition to the satellite toolbox, sea surface salinity, has paved the way for much greater understanding of large-scale air-sea coupling in the Bay of Bengal. This region is replete with mesoscale and submesoscale features and associated surface currents that profoundly impact air-sea heat exchanges and vertical mixing in the ocean. Sea surface height from satellite altimeters is widely used for understanding the dynamics of such features. This article reviews how satellite data are used to monitor and understand various air-sea interactions in the Bay of Bengal and presents a brief overview of modeling efforts underway in this important region.

INTRODUCTION

The Bay of Bengal (BoB) in the Indian Ocean has unique dynamics and thermodynamics. The bay is surrounded by land on three sides and receives freshwater from five of the world's 50 largest rivers: Brahmaputra, Ganges, Irrawaddy, Godavari, and Mahanadi (Sengupta et al., 2006; Papa et al., 2012). BoB dynamics are mainly governed by annually reversing winds from the southwest (i.e., summer monsoon, June to September) and from the northeast (i.e., winter monsoon, November to February). This seasonal change in wind direction results in annual reversal of the upper-ocean current systems. The major current in the BoB flows along its western boundary and is known as the East India Coastal Current (EICC). Though the current's reversal is seasonal, it leads the wind reversal by several months because of remote wind forcing from the equatorial Indian Ocean and the western coast of Myanmar. This remote forcing propagates through the coastal regions of the BoB as coastal Kelvin waves and contributes energy to the EICC (Yu et al., 1991; McCreary et al., 1993).

Local rainfall as well as redistribution of freshwater from rivers freshens the BoB's surface and results in the formation of a barrier layer (a layer between the mixed layer and the isothermal layer; Vinayachandran et al., 2002; Thadathil et al., 2008). The barrier layer prevents vertical mixing and thus modulates sea surface temperature (SST; Masson et al., 2002). Satellite-derived sea surface salinity (SSS) provides additional insight into the formation of barrier layers in the BoB, improving understanding and prediction of the impact of the barrier layer on air-sea interaction.

The BoB remains relatively warm throughout the year and hence contributes to the local climate by supplying heat for monsoon convection. Upper-ocean physical processes such as heat fluxes, advection, and mixing govern SST. In situ ocean observations reveal that apart from temperature, salinity also plays a crucial role in determining the mixed layer depth (MLD) in the tropical ocean (Webster and Lukas, 1992; Bhat et al., 2001; Webster et al., 2002; Wijesekera et al., in press).

Large-scale air-sea coupled processes can be monitored through space-borne synoptic observations from various satellite sensors. With the advent in recent years of operational space-borne and microwave radiometers, the BoB has abundant SST measurements from the Tropical Rainfall Measuring Mission's Microwave Imager (TRMM-TMI), the Advanced Microwave Scanning Radiometer-EOS (AMRS-E), the Advanced Very High Resolution Radiometer (AVHRR), and INSAT-3D (the Indian Space Research Organization's advanced weather satellite), as well as SSS measurements from the Soil Moisture and Ocean Salinity (SMOS), Aquarius, and the Soil Moisture Active Passive (SMAP) satellite sensors. The spatial resolution of such space-borne infrared-based observations is ~1 km; however, such sensors cannot penetrate clouds. Microwave-based sensors provide data under all weather conditions but with a coarser resolution (~25 km). These latter sensors are therefore insufficient to measure submesoscale variability; however, their synoptic coverage helps to monitor basin-scale phenomena.

Short-period SST oscillations during the southwest (summer) monsoon are common in the Indian Ocean, especially in the BoB (Sengupta and Ravichandran, 2001). Parekh et al. (2004) found an 8–16 day period in SST oscillations from TRMM-TMI measurements. These monsoon intraseasonal oscillations (MISOs) are closely linked to the large-scale atmospheric convection associated with the summer monsoon (Yasunari, 1979; Sikka and Gadgil, 1980; Webster et al., 1998).

Intraseasonal variability in cloudiness, as evidenced by decreased outgoing longwave radiation, modulates the shortwave input to the ocean, which results in SST MISOs under low-wind conditions (Agarwal et al., 2007). These kinds of MISOs are generally missing in atmospheric reanalyses due to improper representation of clouds in numerical models (Weare, 1997). Shortwave radiation measurements from satellites are quite useful where there is accurate information about clouds, permitting estimates of radiative forcing (Shahi et al., 2011).

This article gives a general review of the progress that has been made in monitoring the dynamics and thermodynamics of the Bay of Bengal using satellite observations. We focus on satellite-derived parameters, mainly SSS, SST, winds, precipitation, and sea surface height and how their space-time variability modifies air-sea interactions. In situ observations are also used to evaluate satellite-derived SST and SSS in the BoB.

SATELLITE MEASUREMENT OF SSS AND SST: SOURCES AND ASSESSMENT

Prior to 2010, Argo floats, scattered buoys, and ship measurements were the major sources of salinity information. The SMOS mission, launched by the European Space Agency, was a revolution in ocean remote sensing because it carried the first ocean salinity sensor onboard a space platform (Kerr et al., 2010). The salinity measured from this sensor is consistent with observations of the equatorial Indian Ocean (Ratheesh et al., 2013), but due to the larger satellite footprint and land contamination, the errors in SSS are found to be large in the BoB.

In 2011, the US National Aeronautics and Space Administration (NASA) launched Aquarius, with the aim of measuring SSS with an accuracy of 0.2 psu at monthly time scales at a horizontal resolution of 1.5° × 1.5°. The salinity measurements made by Aquarius were found to be much better as compared to those from SMOS. Drucker and Riser (2014) carried out extensive validation of Aquarius salinity data with global Argo floats and found an overall bias of about +0.02 psu. In the BOB, the instrument provides salinity with an accuracy of 0.5 psu (Ratheesh et al., 2014) and nicely reproduces the spatial patterns found in Argo data.

Aquarius was declared nonfunctional in May 2015, once again leaving a huge void in salinity measurements over the global ocean. Since April 2015, SSS data from NASA's SMAP sensor can be obtained from http://www.remss.com/missions/smap (Meissner et al., 2015). These data sets are available as eight-day running averages or monthly averaged fields. Figure 1 shows a plot of SSS from SMAP averaged for August 21–September 18, 2015, in the BoB. During this time, in situ salinity measurements in the Bay of Bengal taken by a thermosalinograph were available from an R/V *Roger Revelle* cruise conducted under the joint US Air-Sea Interactions Regional Initiative (ASIRI) and Indian Ocean Mixing and Monsoon (OMM) program (Lucas et al., 2016, in this issue; Wijesekera et al., in press). Figure 1 shows the observations along the ship's track overlaid on SMAP salinity. Freshening observed along the ship's track in the northern BoB is missing from the satellite data. This mismatch could be due to the fact that the salinity from SMAP is averaged over the cruise period while the ship observations are instantaneous. Although the onboard radar failed, the quality of SMAP data is promising, and we hope that the challenge of measuring SSS from space is being overcome with such missions.

Several satellite imagers have routinely provided SST for decades. The US National Oceanic and Atmospheric

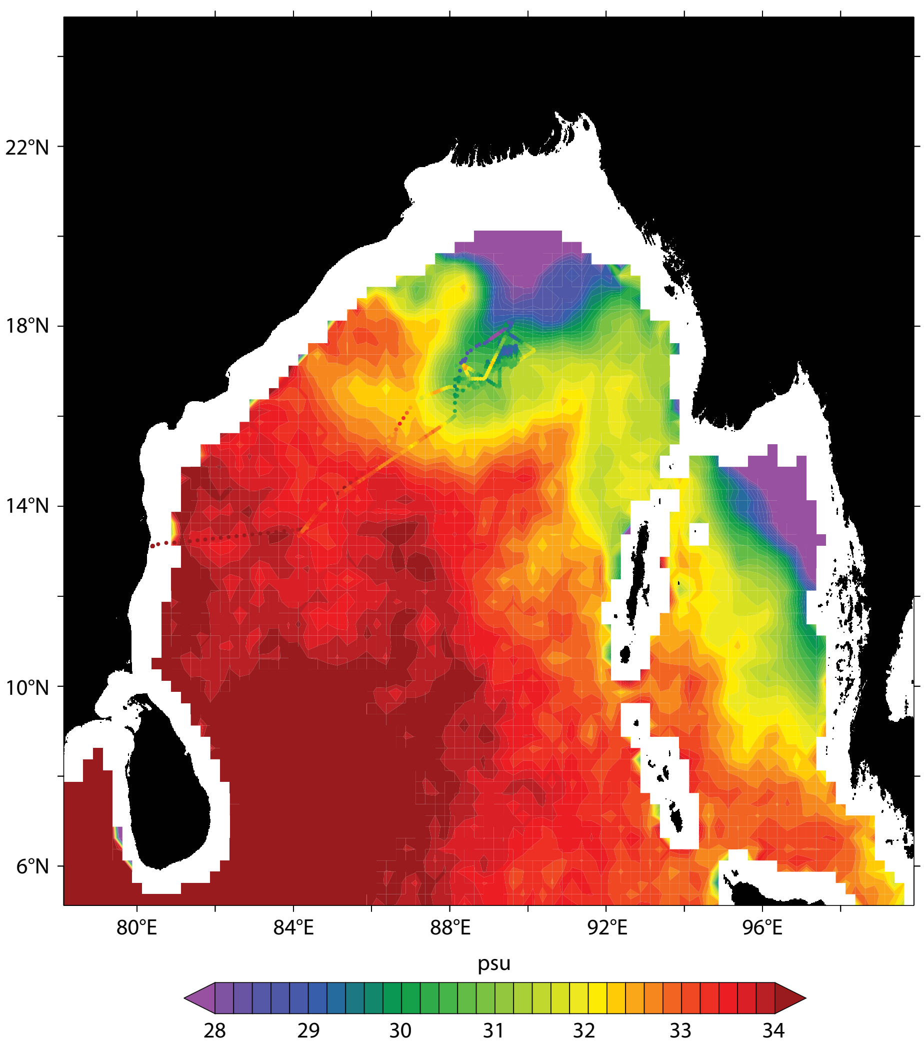

FIGURE 1. Sea surface salinity from the Soil Moisture Active Passive (SMAP) satellite averaged over August–September 2015. Sea surface salinity measured from a thermosalinograph deployed from R/V *Roger Revelle* during its cruise from August to September 2015 is overlaid.

Administration's (NOAA's) series of AVHRRs and the NASA's Moderate Resolution Imaging Spectroradiometer (MODIS) provide infrared-based high-resolution SST that is used in many applications such as fisheries (Solanki et al., 2015) and air-sea interaction studies (Chelton and Xie, 2010). These infrared sensors provide information only under clear sky conditions; however, with the availability of microwave sensors, SST can be derived under all weather conditions (albeit with lower spatial resolution). The Group of High Resolution Sea Surface Temperature (GHRSST) data available from the Jet Propulsion Laboratory (JPL; ftp://mariana.jpl.nasa.gov/mur_sst/tmchin/docs/ATBD) is a merged SST product that includes SST from all the available microwave and infrared sensors. The Level-4 product is generated using various objective analysis techniques to produce gap-free SST maps over the global ocean. This product ensures 100% coverage of the global ocean on daily time scales. We compared GHRSST data with data from two Research Moored Array for African-Asian-Australian Monsoon Analysis and Prediction (RAMA) buoys (McPhaden et al., 2009) located along 90°E at 12°N and 15°N in the BOB. The range and variability of GHRSST correctly reproduces the observations. The coefficient of determination is 0.93 and 0.95, respectively, at these two locations, and the root mean square error (RMSE) is 0.35°C at both locations. Since the product is at 1 km × 1 km spatial resolution (mainly under cloud-free conditions), it is very useful for tracking and understanding mesoscale features in the ocean.

SEASONAL VARIABILITY

Mean SSS in the BoB between 2012 and 2014 from Aquarius (CAP version 4.0 data; ftp://podaac-ftp.jpl.nasa.gov/allData/aquarius/L2/CAPv4) exhibits lower values (less than 29 psu) in the northernmost region of the BoB (Figure 2a) as a result of heavy river discharge from the Ganges-Brahmaputra and Irrawaddy Rivers (Papa et al., 2012). Runoff from these rivers is seasonal, maximum during the summer monsoon and minimum (around 1–2 psu) during the winter monsoon, leading to high SSS variability in this region (Figure 2b). The southern part of the BoB is more saline due to excessive tropical evaporation and advection of saltier waters from the equatorial Indian Ocean (Jensen et al., 2016, this issue). SSS in the central and southern BoB is more uniform than in the northern BoB (Figure 2a). Figure 3 displays the large seasonal variation in SSS in the BoB for January and July 2012 to 2014. These data show that the northern BoB has lower SSS values in January as compared to July due to maximum influx of freshwater from August to September resulting from heavy river discharge (Papa et al., 2012). Mesoscale eddies distribute these low-salinity waters southward over the course of several months.

Rainfall over the BoB also occurs with a seasonal pattern associated with the southwest (summer) and northeast (winter) monsoons (Figure 4). Warm, moist equatorial flow during the southwest monsoon results in the most intense rainfall during this time period (Webster et al., 1998). Although a secondary period of rainfall occurs during the northeast monsoon, dry continental air advected by the northeast winds typically results in less intense and less widespread rainfall (Kripalani and Kumar, 2004). Rainfall during other times of the year is sparse. Remote sensing offers the advantage of high spatial and consistent temporal coverage of rainfall, allowing measurement of its seasonal occurrence over the BoB. In particular, the TMI sensor on the TRMM satellite provided unprecedented measurements of tropical rainfall for more than 15 years (1997–2014; Wentz et al., 2015). These data (Figure 4) show a significant west

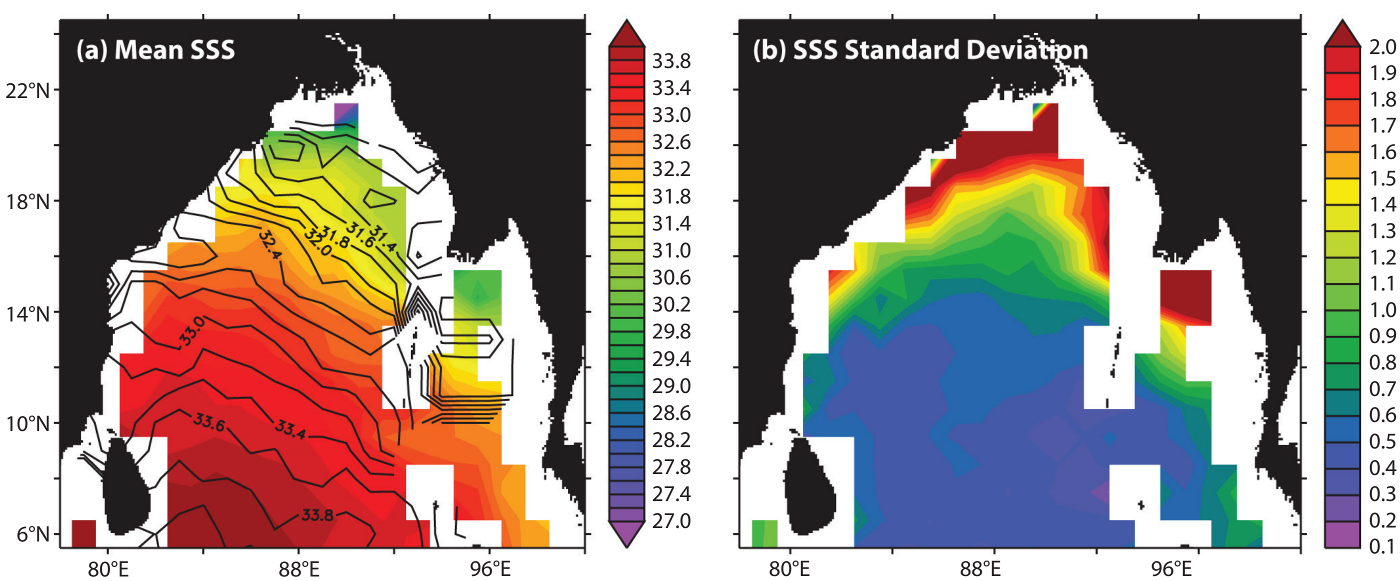

FIGURE 2. (a) Sea surface salinity (SSS) from the Aquarius satellite averaged over 2012–2014. Contours of sea surface salinity from Argo floats averaged over the same period are overlaid. (b) Standard deviation of sea surface salinity for the period 2012–2014.

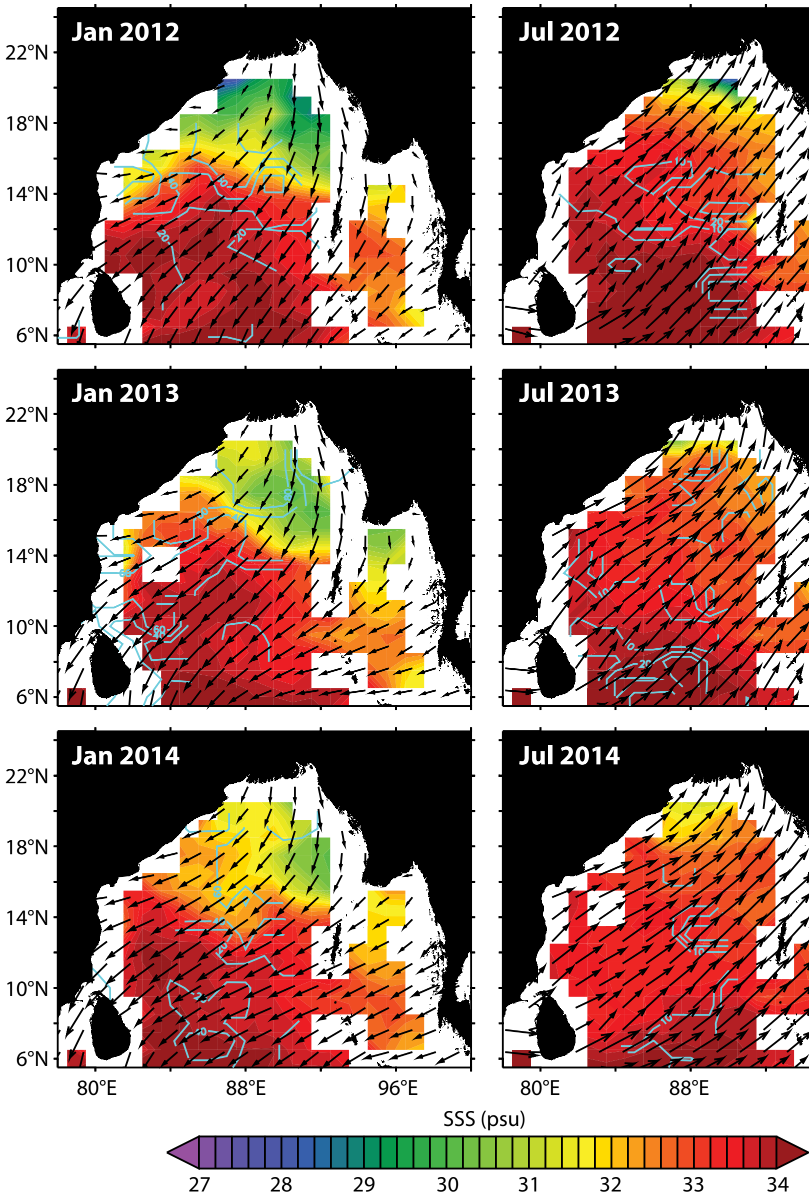

FIGURE 3. Sea surface salinity (shaded, psu) and sea surface winds (vector, m s^{-1}) averaged for January (left) and July (right) for 2012 (top), 2013 (middle), and 2014 (bottom). Contours of barrier layer thickness (m) are shown in cyan. SSS data are from Aquarius (CAP version 4.0 data; ftp://podaac-ftp.jpl.nasa.gov/allData/aquarius/L2/CAPv4). Wind data are from ERA-Interim reanalysis (Dee et al., 2011).

to east gradient in the annual distribution of rainfall. This gradient is the result of the southwest monsoon winds carrying moist air toward the eastern BoB (west coast of Myanmar), where coastal and orographic effects trigger rainfall (Kumar et al., 2014). The western BoB (east coast of India) does not experience similarly large amounts of coastal rainfall. During the southwest monsoon, the western BoB is in the lee (downwind) of India's Western Ghats mountains, resulting in reduced rainfall amounts in summer (Kripalani and Kumar, 2004; Kumar et al., 2014). Rainfall along the east coast of India during the southwest monsoon typically results from rain bands that form to the south and propagate northwestward (Gadgil, 2003). Atmospheric flow during the northeast monsoon brings rainfall to the east coast of India during winter, but dry continental air advected by northeast winds results in less winter rainfall in this region than in the summer

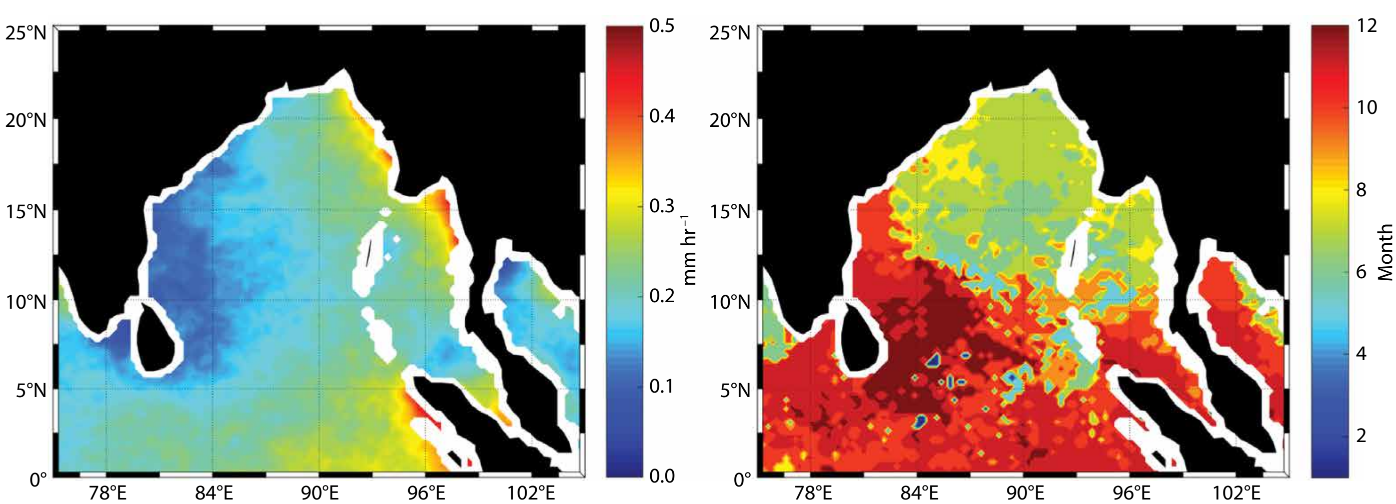

FIGURE 4. Annual rainfall distribution derived from Tropical Rainfall Measuring Mission's Microwave Imager (TRMM-TMI) data (1998–2014). (left) The annual average rain rate (mm h^{-1}) in the BoB. (right) The month of the year (January = 1, December = 12) where the monthly average rainfall is a maximum.

over the west coast of Myanmar. This seasonality results in the maximum rainfall over the northern BoB during the summer months, and the maximum rainfall over the southern BoB during the winter months, after the seasonal winds become northeasterly (Figure 4).

Intense rainfall in the northern BoB during the summer months has important implications for upper-ocean stratification in this region. The enormous influx of freshwater from the Ganges-Brahmaputra river system in the northern BoB during the summer months affects upper-ocean stratification, particularly with regard to barrier layer thickness. The area of most intense summer rainfall occurs just to the southeast of the mouth of this river system, providing additional freshwater to the far northern BoB. This spatial and temporal coherence of both sources of freshwater add to the intensity of the annual freshwater plume, highlighting the importance of understanding the role this freshwater plays in air-sea interactions.

INTERANNUAL VARIABILITY

Among the three years (2012–2014) studied, the January salinity distribution in the northern BoB (north of 14°N) is lowest in 2012 (Figure 3). A north-south salinity gradient in the northern bay during January is prominent in 2012 and 2013, while 2014 has a clear east-west gradient. The surface freshening in January 2012 captured by Aquarius was also reported by Pant et al. (2015) using Argo float observations. They attributed enhanced monsoon precipitation and a positive Indian Ocean Dipole followed by a weaker EICC for this freshening during winter 2012. The SSS pattern in July 2012 shows more freshening in the northern BoB compared to July 2013 and 2014 (Figure 3). The strength of freshening in the northern BoB has a direct impact on the interaction between the atmosphere and the upper ocean as it sets up a barrier layer. The barrier layer thickness (BLT) magnitude (shown as cyan contours in Figure 3) is shallower in the northern BoB where the salinity is low compared to the central and southern BoB. BLT, defined as the difference between isothermal layer depth (ILD) and MLD, is computed using individual Argo profiles following the methodology used by Agarwal et al. (2012), and it is then averaged in a 1° × 1° box for each month. BLT is quite large (~80 m) around 18°N in January of 2012 and 2013, while during 2014 it remained <60 m in this region. During July, BLT varied between 10 m and 30 m in the entire basin. Sea surface winds in the northern BoB are much higher during July than in January, providing more kinetic energy (Agarwal et al., 2012) during July for breaking the barrier layer, which results in thin BLTs. Interannual variability in winds is one of the factors responsible for salinity and BLT variability. This is evident in January 2014 when the winds are higher in the northern BoB, resulting in enhanced vertical mixing, and leading to thinner BLTs compared to 2012 and 2013.

SST averaged for January and July 2012–2014 (Figure 5) shows significant cooling in the BoB in January 2014, with temperatures ≤27°C north of 10°N. Winds were strongest in 2014 among

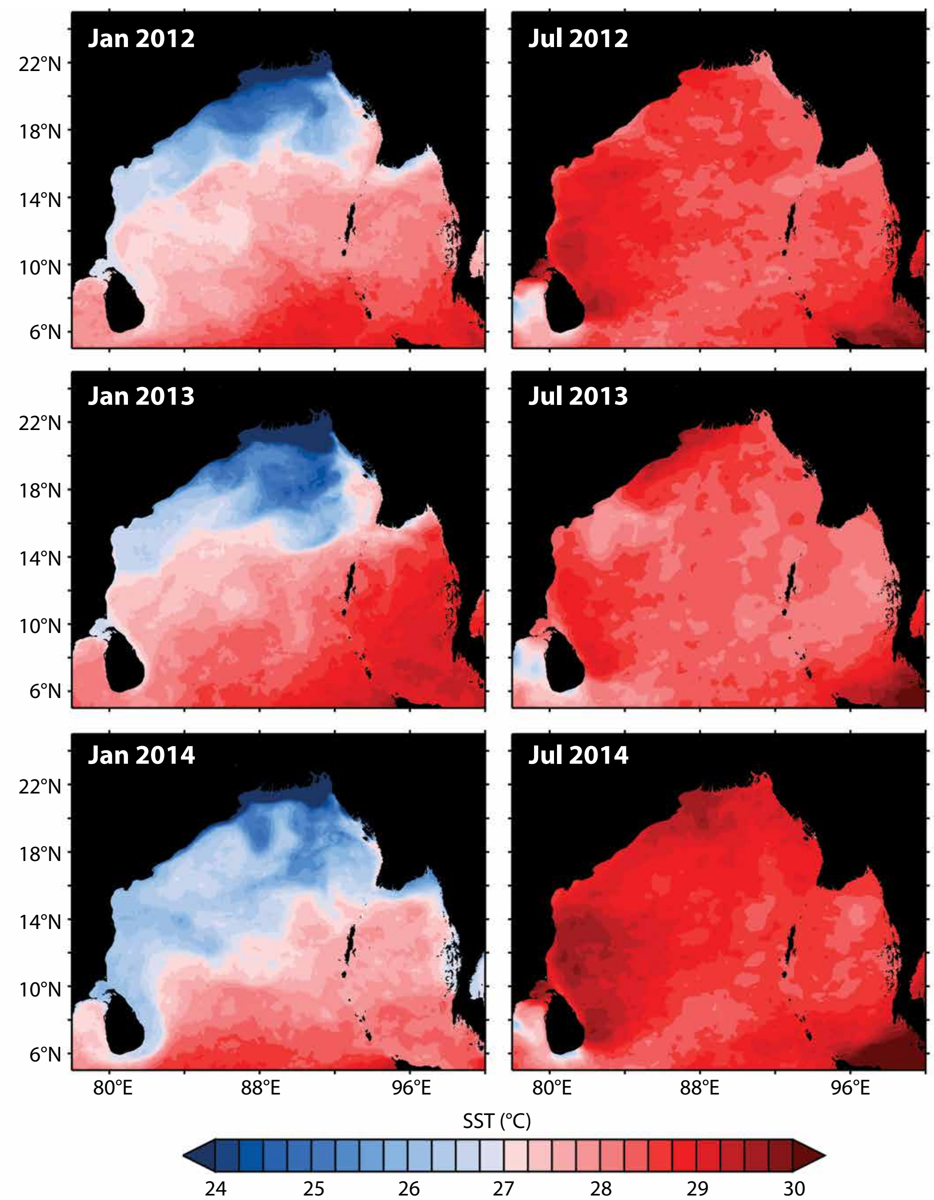

FIGURE 5. Sea surface temperature (shaded, °C) for January (left) and July (right) for 2012 (top), 2013 (middle), and 2014 (bottom).

these three years (Figure 3), indicating latent heat loss from the ocean to the atmosphere. Cooling in the BoB north of 18°N is larger in 2012 and 2013 compared to 2014 (Figure 5). Weaker winds and lower salinity caused the cooling to be confined to the top layer of the ocean in this region, resulting in lower SSTs. The latent heat released into the atmosphere during 2012 and 2013 was lower than during 2014 in the northern BoB (figure not shown). SST in the entire BoB remained quite warm during July, varying between 28.5°C and 29.5°C.

Slight deviations are seen in the central BoB in July 2013 when cooling is evident at 15°N near the east coast of India. The cause of this cooling does not seem to be related to the winds, which are similar to the other two years.

Sea surface height anomaly data available from space-borne altimeters provides a rich source of information about mesoscale eddies in the BoB. Large-scale currents in the BoB are predominantly geostrophic and can be computed from these data. The Aviso merged altimeter product provides daily maps of analyzed sea surface height anomalies and geostrophic currents in the BoB. Figure 6 shows that eddies in both winter and summer months dominate the BoB. The geostrophic currents in the BoB stir the anomalously low-salinity water, helping to set the BLT and modulate air-sea interactions.

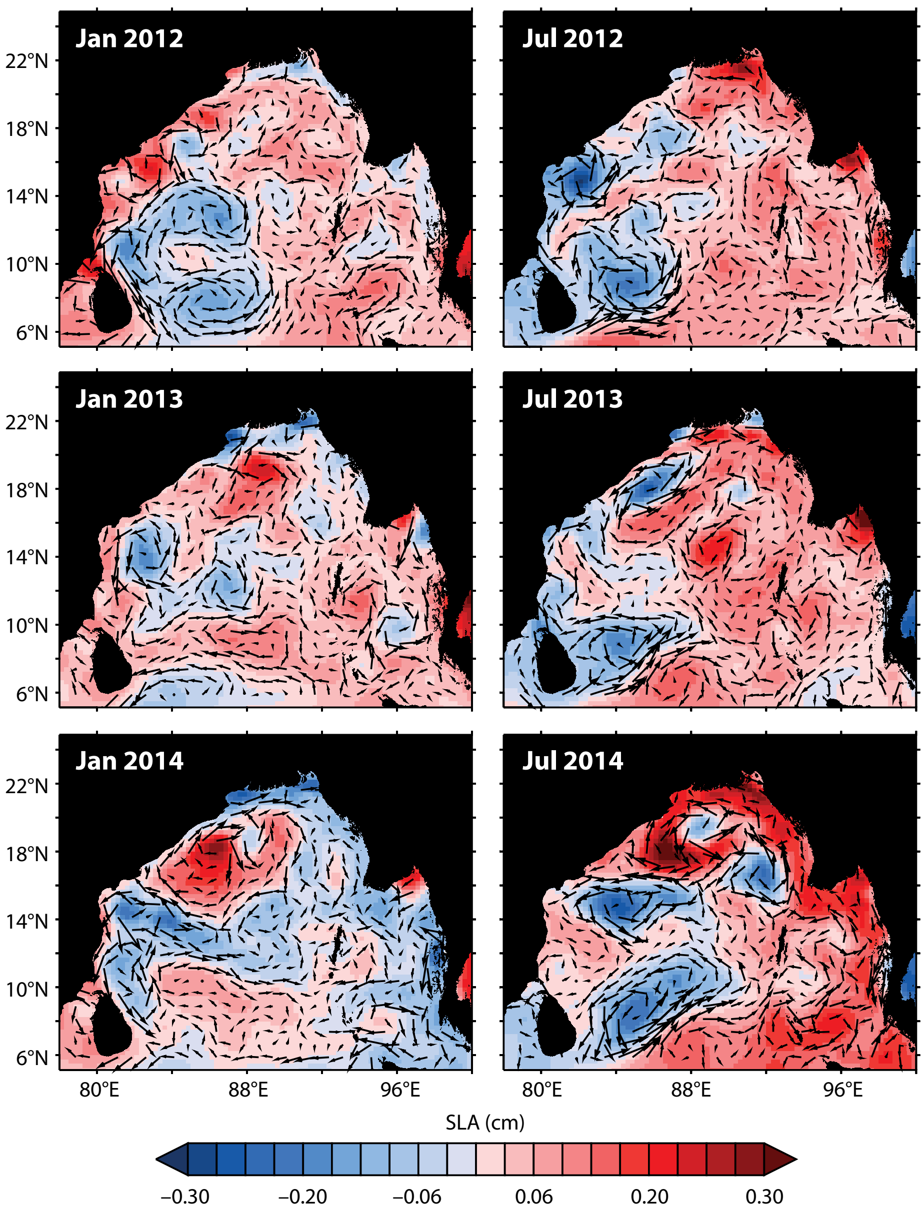

FIGURE 6. Sea surface height anomaly (m) from the Aviso merged product overlaid with geostrophic currents (m s^{-1}) for January (left) and July (right) for 2012 (top), 2013 (middle), and 2014 (bottom).

THERMAL FRONTS

Remote observations of thermal fronts are important to the fishing industry, as regions of strong thermal gradients are associated with strong vertical movement of nutrients and thus higher phytoplankton biomass (Marra et al., 1990). Additionally, thermal fronts can modulate heat exchange with the atmosphere, which can alter the tracks of tropical cyclones (Yu and McPhaden, 2011). Large-scale thermal gradients are computed using the methodology of Kostianoy et al. (2004) at every grid point in the BoB for the month of January during 2012–2014 using monthly averaged GHRSST analysis. Only thermal gradients greater than 0.02°C km^{-1} are considered. GHRSST data show that sharp thermal gradients occur in the northern BOB (north of 15°N). Most of these fronts propagate offshore. Large gradient values suggestive of strong fronts have preferred formation locations along the east coast of India, north of 20.50°N, and toward the eastern side of the BoB along the coast of Myanmar (Figure 7). These preferred regions are at shelf breaks, suggesting bottom topography plays a role in the formation of these fronts. Frontal activity is stronger during winter months (November to April), with maximum gradients (~0.08–0.1°C km^{-1}) during January. There are three prominent fronts in January in this region. Thermal gradients more than 0.02°C km^{-1} are not observed during July in this product. July winds are quite strong and uniform and result in basin-wide mixing of the ocean. This could be one reason that the thermal gradients are weaker than 0.02°C km^{-1} during this period, as strong winds tend to create a more homogenous basin. However, we must exercise caution in the interpretation of thermal fronts during the southwest monsoon season (June to September). Due to cloud cover during this period, GHRSST primarily has microwave SST contributions. The microwave measurements normally have a large footprint (>25 km), and most of the SST fields are smoothed, so small-scale features cannot be resolved. Therefore, it is still unknown whether strong monsoonal winds and consequent mixing inhibits the fronts or whether we are unable to detect these fronts due to limitations of the data set.

Interannual variability of fine-scale thermal gradients is associated with large-scale variability of sea surface winds, SSS, and basin-scale eddy activity. Although the region where these gradients are found lies in the vicinity of river discharge, the variability of thermal gradients does not directly correlate with the strength of the discharge, since the thermal gradients are weaker in January 2012 compared to 2013 and 2014. The northern BoB experienced weaker northerly winds, significant freshening (Figure 3), and weak eddy activity (Figure 5) during January 2012. Despite the strong stratification due to higher discharge, the weak winds and low eddy activity sustained the weaker thermal gradients and low frontal activity. The formation of thermal fronts seems to require strong spatial variability in stratification, along with strong eddy stirring.

SUMMARY AND PATH FORWARD

Remotely sensed observations of SST, sea surface height, winds, and precipitation were used to study air-sea interactions over the Bay of Bengal. Since 2009, SSS observations from space have precipitated a giant leap in understanding of this data-sparse region. A thick barrier layer dominates the low-salinity regions during the winter months, restricting air-sea interaction to a shallow upper-ocean layer in the BoB. Interannual variability in winds, mesoscale eddies, and enormous freshwater influx are the main contributors to SSS and SST variability in this region. Fine-scale thermal and salinity gradients also dominate the region. Thermal gradients monitored using high-resolution satellite SST show strong interannual variability, which is mainly influenced by variability in salinity and wind.

Although satellite data provide synoptic coverage of mesoscale, and to some extent submesoscale, features (MacKinnon et al., 2016, in this issue), interest remains in obtaining information about the dynamics of these features at high resolution during monsoon seasons. In order to get fine-scale information during monsoon months, researchers mainly rely on numerical ocean models and small-scale process studies using data obtained from ships (Hormann et al., 2016, in this issue; Wijesekera et al., in press). With increasing computational power, numerical models are now capable of providing simulations at extremely high spatial (both horizontal and vertical) resolution. A state-of-the-art operational model run at the US Naval Research Laboratory (see Jensen et al., 2016, in this issue) provides near-real-time ocean information at 1/12° × 1/12°. These models are mainly used for operational

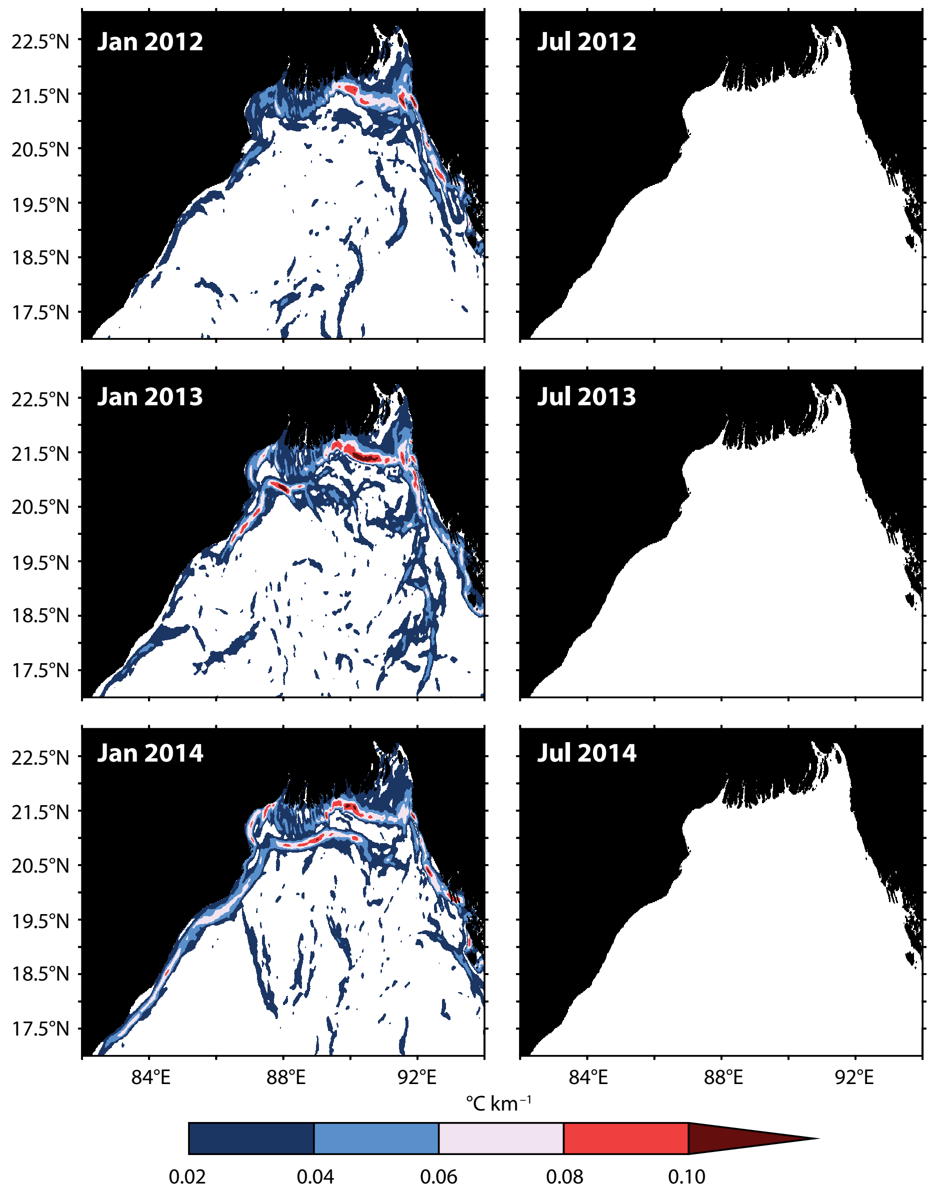

FIGURE 7. Contours of SST gradients (°C km^{-1}) for January (left) and July (right) for 2012 (top), 2013 (middle), and 2014 (bottom). Gradients ≤0.02°C km^{-1} are shaded white.

purposes, and they are constrained by in situ and satellite observations using various data assimilation techniques.

Several aspects of the Bay of Bengal, such as the SST MISO mechanism, barrier layer formation, eddy-driven circulation, and mixing have been addressed using numerical models (Sharma et al., 2010; Chowdary et al., 2015; Fousiya et al., 2015). These ocean models perform well when forced with accurate fluxes of momentum, heat, and freshwater (Agarwal et al., 2007). Most of the numerical models without data assimilation fail to accurately represent the BoB despite performing well in equatorial regions and also in the regions where winds play a dominant role in ocean circulation (Fousiya et al., 2015). Although prescription of accurate momentum and radiative fluxes to force boundaries has helped to improve large-scale ocean circulation and air-sea interactions (such as the MISOs) in the models (Agarwal et al., 2007), accurate simulation of salinity stratification and vertical mixing in this region remains a challenge (Goswami et al., 2016, in this issue).

Considering the importance of satellite observations in providing a synoptic view of oceanic features and associated large-scale air-sea interaction, it would be highly desirable to have frequent observations (about half-hourly) of SST with high spatial resolution (of the order of a few kilometers). These measurements are possible only with a satellite in a geostationary orbit. In this regard, the Indian satellites, INSAT-3D and the forthcoming INSAT-3DR, along with the Geostationary Hyperspectral Imager Satellite (GISAT), hold promise. Computing large-scale air-sea heat exchange will also need accurate surface wind observations from satellites. The large-swath scatterometer, SCATSAT-1, planned by the Indian Space Research Organization, will be highly useful in this study. Two well-calibrated salinity missions that would provide frequent data (approximately every three days) would help to understand stratification in the Bay of Bengal. Sea surface height data from three to four nadir-viewing altimeters would be desirable as this region is rich in mesoscale features. A forthcoming French-American swath altimetry mission called Surface Water and Ocean Topography (SWOT) will provide a synoptic view of submesoscale features.

REFERENCES

Agarwal, N., R. Sharma, S. Basu, A. Parekh, A. Sarkar, and V.K. Agarwal. 2007. Bay of Bengal summer monsoon 10–20 day variability in sea surface temperature using model and observations. *Geophysical Research Letters* 34, L06602, http://dx.doi.org/10.1029/2007GL029296.

Agarwal, N., R. Sharma, S. Basu, A. Parekh, A. Sarkar, and V.K. Agarwal. 2012. Argo observations of barrier layer in the tropical Indian Ocean. *Advances in Space Research* 50(5):642–654, http://dx.doi.org/10.1016/j.asr.2012.05.021.

Bhat, G.S., S. Gadgil, P.V. Hareesh Kumar, S.R. Kalsi, P. Madhusoodanan, V.S.N. Murty, C.V.K. Prasada Rao, V. Ramesh Babu, L.V.G. Rao, R.R. Rao, and others. 2001. BOBMEX: The Bay of Bengal Monsoon Experiment. *Bulletin of the American Meteorological Society*, 20(10):2,217–2,243, http://dx.doi.org/10.1175/1520-0477(2001)082<2217:BTBOBM>2.3.CO;2.

Chelton, D.B., and S.-P. Xie. 2010. Coupled ocean–atmosphere interaction at oceanic mesoscales. *Oceanography* 23(4):52–69, http://dx.doi.org/10.5670/oceanog.2010.05.

Chowdary, J.S., A. Parekh, S. Ojha, and C. Gnanaseelan. 2015. Role of upper ocean processes in the seasonal SST evolution over tropical Indian Ocean in climate forecasting system. *Climate Dynamics* 45:2,387–2,405, http://dx.doi.org/10.1007/s00382-015-2478-4.

Dee, D.P., S.M. Uppala, A.J. Simmons, P. Berrisford, P. Poli, S. Kobayashi, U. Andrae, M.A. Balmaseda, G. Balsamo, P. Bauer, and others. 2011. The ERA-Interim reanalysis: Configuration and performance of the data assimilation system. *Quarterly Journal of the Royal Meteorological Society* 137:553–597, http://dx.doi.org/10.1002/qj.828.

Drucker, R., and S.C. Riser. 2014. Validation of Aquarius sea surface salinity with Argo: Analysis of error due to depth of measurement and vertical salinity stratification. *Journal of Geophysical Research* 119(7):4,626–4,637, http://dx.doi.org/10.1002/2014JC010045.

Fousiya, T.S., A. Parekh, and C. Gnanaseelan. 2015. Interannual variability of upper ocean stratification in Bay of Bengal: Observational and modeling aspects. *Theoretical and Applied Climatology*, http://dx.doi.org/10.1007/s00704-015-1574-z.

Gadgil, S. 2003. The Indian monsoon and its variability. *Annual Review of Earth and Planetary Sciences* 31:429–467, http://dx.doi.org/10.1146/annurev.earth.31.100901.141251.

Goswami, B.N., S.A. Rao, D. Sengupta, and S. Chakravorty. 2016. Monsoons to mixing in the Bay of Bengal: Multiscale air-sea interactions and monsoon predictability. *Oceanography* 29(2):18–27, http://dx.doi.org/10.5670/oceanog.2016.35.

Hormann, V., L.R. Centurioni, A. Mahadevan, S. Essink, E.A. D'Asaro, and B. Praveen Kumar. 2016. Variability of near-surface circulation and sea surface salinity observed from Lagrangian drifters in the northern Bay of Bengal during the waning 2015 southwest monsoon. *Oceanography* 29(2):124–133, http://dx.doi.org/10.5670/oceanog.2016.45.

Jensen, T.G., H.W. Wijesekera, E.S. Nyadjro, P.G. Thoppil, J.F. Shriver, K.K. Sandeep, and V. Pant. 2016. Modeling salinity exchanges between the equatorial Indian Ocean and the Bay of Bengal. *Oceanography* 29(2):92–101, http://dx.doi.org/10.5670/oceanog.2016.42.

Kerr, Y.H., P. Waldteufel, J.P. Wigneron, S. Delwart, F. Cabot, J. Boutin, M.J. Escorihuela, J. Font, N. Reul, C. Gruhier, and others. 2010. The SMOS mission: New tool for monitoring key elements of the global water cycle. *Proceedings of the IEEE* 98(5):666–687, http://dx.doi.org/10.1109/JPROC.2010.2043032.

Kostianoy, A.G., A.I. Ginzburg, M. Frankignoulle, and B. Delille. 2004. Fronts in the southern Indian Ocean as inferred from satellite sea surface temperature data. *Journal of Marine Systems* 45:55–73, http://dx.doi.org/10.1016/j.jmarsys.2003.09.004.

Kumar, S., A. Hazra, and B.N. Goswami. 2014. Role of interaction between dynamics, thermodynamics and cloud microphysics on summer monsoon precipitating clouds over the Myanmar coast and the western Ghats. *Climate Dynamics* 43(3):911–924, http://dx.doi.org/10.1007/s00382-013-1909-3.

Kripalani, R.H., and P. Kumar. 2004. Northeast monsoon rainfall variability over south peninsular India vis-à-vis the Indian Ocean dipole mode. *International Journal of Climatology* 24:1,267–1,282, http://dx.doi.org/10.1002/joc.1071.

Lucas, A.J., J.D. Nash, R. Pinkel, J.A. MacKinnon, A. Tandon, A. Mahadevan, M.M. Omand, M. Freilich, D. Sengupta, M. Ravichandran, and A. Le Boyer. 2016. Adrift upon a salinity-stratified sea: A view of upper-ocean processes in the Bay of Bengal during the southwest monsoon. *Oceanography* 29(2):134–145, http://dx.doi.org/10.5670/oceanog.2016.46.

MacKinnon, J.A., J.D. Nash, M.H. Alford, A.J. Lucas, J.B. Mickett, E.L. Shroyer, A.F. Waterhouse, A. Tandon, D. Sengupta, A. Mahadevan, and others. 2016. A tale of two spicy seas. *Oceanography* 29(2):50–61, http://dx.doi.org/10.5670/oceanog.2016.38.

Marra, J., R.W. Houghton, and C. Garside. 1990. Phytoplankton growth at the shelf-break front in the Middle Atlantic Bight. *Journal of Marine Research* 48(4):851–868.

Masson, S., P. Delecluse, J.P. Boulanger, and C. Menkes. 2002. A model study of the seasonal variability and formation mechanisms of barrier layer in the eastern equatorial Indian Ocean. *Journal of Geophysical Research* 107(C12), 8017, http://dx.doi.org/10.1029/2001JC000832.

McCreary, J.P., P.K. Kundu, and R.L. Molinari. 1993. A numerical investigation of the dynamics, thermodynamics and mixed-layer processes in the Indian Ocean. *Progress in Oceanography* 31:181–244, http://dx.doi.org/10.1016/0079-6611(93)90002-U.

McPhaden, M.J., G. Meyers, K. Ando, Y. Masumoto, V.S.N. Murty, M. Ravichandran, F. Syamsudin, J. Vialard, L. Yu, and W. Yu. 2009. RAMA: The Research Moored Array for African-Asian-Australian Monsoon Analysis and Prediction. *Bulletin of the American Meteorological Society* 90:459–480, http://dx.doi.org/10.1175/2008BAMS2608.1.

Meissner, T., F.J. Wentz, D. Le Vine, and P. de Matthaeis. 2015. *Addendum IV to ATBD*. RSS Technical Report 071515, 16 pp., ftp://podaac.jpl.nasa.gov/allData/aquarius/docs/v4/AQ-014-PS-0017_AquariusATBD_Level2_Addendum4_DatasetVersion4.0.pdf.

Pant, V., M.S. Girishkumar, T.V.S. UdayaBhaskar, M. Ravichandran, F. Papa, and V.P. Thangaprakash. 2015. Observed interannual variability of near surface salinity in the Bay of Bengal. *Journal of Geophysical Research* 120(5):3,315–3,329, http://dx.doi.org/10.1002/2014JC010340.

Papa, F., S.K. Bala, R.K. Pandey, F. Durand, V.V. Gopalakrishna, A. Rahman, and W.B. Rossow. 2012. Ganga-Brahmaputra river discharge from Jason-2 radar altimetry: An update to the long-term satellite-derived estimates of continental freshwater forcing flux into the Bay of Bengal. *Journal of Geophysical Research* 117, C11021, http://dx.doi.org/10.1029/2012JC008158.

Parekh, A., A. Sarkar, S. Shah, and M.S. Narayanan. 2004. Low period variability in Tropical Rainfall Measuring Mission Microwave Imager measured sea surface temperature over the Bay of Bengal during monsoon. *Current Science* 87:791–796.

Ratheesh, S., B. Mankad, S. Basu, R. Kumar, and R. Sharma. 2013. Assessment of satellite-derived sea surface salinity in the Indian Ocean. *IEEE Geoscience and Remote Sensing Letters* 10(3):428–431, http://dx.doi.org/10.1109/LGRS.2012.2207943.

Ratheesh, S., R. Sharma, and S. Basu. 2014. An EnOI assimilation of satellite data in an Indian Ocean circulation model. *IEEE Transactions on Geoscience Remote Sensing* 52:4,106–4,111, http://dx.doi.org/10.1109/TGRS.2013.2279606.

Sengupta, D., G.N. Bharath Raj, and S.S.C. Shenoi. 2006. Surface freshwater from Bay of Bengal runoff and Indonesian Throughflow in the tropical Indian Ocean. *Geophysical Research Letters* 33, L22609, http://dx.doi.org/10.1029/2006GL027573.

Sengupta, D., and M. Ravichandran. 2001. Oscillations of Bay of Bengal Sea surface temperature during the 1998 summer monsoon. *Geophysical Research Letters* 28(10):2,033–2,036, http://dx.doi.org/10.1029/2000GL012548.

Shahi, N.R., P.K. Thapliyal, R. Sharma, P.K. Pal, and A. Sarkar. 2011. Estimation of net surface shortwave radiation over the tropical Indian Ocean using geostationary satellite observations: Algorithm and validation. *Journal of Geophysical Research* 116, C09031, http://dx.doi.org/10.1029/2011JC007105.

Sharma, R., N. Agarwal, I.M. Momin, S. Basu, and V.K. Agarwal. 2010. Simulated sea surface salinity variability in the tropical Indian Ocean. *Journal of Climate* 23(24):6,542–6,554, http://dx.doi.org/10.1175/2010JCLI3721.1.

Sikka, D.R., and S. Gadgil. 1980. On the maximum cloud zone and the ITCZ over Indian longitudes during the southwest monsoon. *Monthly Weather Review* 108:1,840–1,853, http://dx.doi.org/10.1175/1520-0493(1980)108<1840:OTMCZA>2.0.CO;2.

Solanki, H.U., D. Bhatpuria, and P. Chauhan. 2015. Signature analysis of satellite derived SSHa, SST and chlorophyll concentration and their linkage with marine fishery resources. *Journal of Marine Systems* 150:12–21, http://dx.doi.org/10.1016/j.jmarsys.2015.05.004.

Thadathil, P., P. Thoppil, R.R. Rao, P.M. Muraleedharan, Y.K. Somayajulu, V.V. Gopalakrishna, R. Murtugudde, G.V. Reddy, and C. Revichandran. 2008. Seasonal variability of the observed barrier layer in the Arabian Sea. *Journal of Physical Oceanography* 38:624–638, http://dx.doi.org/10.1175/2007JPO3798.1.

Vinayachandran, P.N., V.S.N. Murty, and V.R. Babu. 2002. Observations of barrier layer formation in the Bay of Bengal during summer monsoon. *Journal of Geophysical Research* 107(C12), 8018, http://dx.doi.org/10.1029/2001JC000831.

Weare, B.C. 1997. Comparison of NCEP–NCAR cloud radiative forcing reanalyses with observations. *Journal of Climate* 10:2,200–2,209, http://dx.doi.org/10.1175/1520-0442(1997)010<2200:CONNCR>2.0.CO;2.

Webster, P.J., E.F. Bradley, C.W. Fairall, and J.S. Godfrey. 2002. The JASMINE pilot study. *Bulletin of the American Meteorological Society* 83(11), http://dx.doi.org/10.1175/BAMS-83-11-1603.

Webster, P.J., and R. Lukas. 1992. TOGA COARE: The Coupled Ocean–Atmosphere Response Experiment. *Bulletin of the American Meteorological Society* 73:1,377–1,416, http://dx.doi.org/10.1175/1520-0477(1992)073<1377:TCTCOR>2.0.CO;2.

Webster, P.J., V.O. Magana, T.N. Palmer, J. Shukla, R.A. Tomas, M. Yanai, and T. Yasunari. 1998. Monsoons: Processes, predictability, and the prospects for prediction. *Journal of Geophysical Research* 103:14,451–14,510, http://dx.doi.org/10.1029/97JC02719.

Wentz, F.J., C. Gentemann, and K.A. Hilburn. 2015. Remote Sensing Systems TRMM TMI weekly Environmental Suite on 0.25 deg grid, Version 7.1. Remote Sensing Systems, Santa Rosa, CA, http://www.remss.com/missions/tmi.

Wijesekera, H.W., E. Shroyer, A. Tandon, M. Ravichandran, D. Sengupta, S.U.P. Jinadasa, H.J.S. Fernando, N. Agarwal, K. Arulanathan, G.S. Bhat, and others. In press. ASIRI: An Ocean-Atmosphere Initiative for Bay of Bengal. *Bulletin of the American Meteorological Society*, http://dx.doi.org/10.1175/BAMS-D-14-00197.1.

Yasunari, T. 1979. Cloudiness fluctuations associated with the Northern Hemisphere summer monsoon. *Journal of the Meteorological Society of Japan* 57:227–242.

Yu, L., and M.J. McPhaden. 2011. Ocean preconditioning of Cyclone Nargis in the Bay of Bengal: Interaction between Rossby waves, surface fresh waters, and sea surface temperatures. *Journal of Physical Oceanography* 41(9):1,741–1,755, http://dx.doi.org/10.1175/2011JPO4437.1.

Yu, L., J.J. O'Brien, and J. Yang. 1991. On the remote forcing of the circulation in the Bay of Bengal. *Journal of Geophysical Research* 96(C11):20,449–20,454, http://dx.doi.org/10.1029/91JC02424.

ACKNOWLEDGMENTS

We are grateful to the Director, Space Applications Centre, Ahmedabad, for his encouragement and support for participating in the ship cruises. We thank Debasis Sengupta for his valuable suggestions. We thank the Indian National Centre for Ocean Information Services (INCOIS) and the National Institute of Ocean Technology (NIOT), Ministry of Earth Sciences (MoES), for providing the required data for this research. This work has been supported by the MoES, India, under the Ocean Mixing and Monsoon (OMM) project. JB and AT were supported by Office of Naval Research grants N00014-14-1-0496 and N00014-13-1-0456.

AUTHORS

R. Sharma (rashmi@sac.isro.gov.in) is Head, Oceanic Sciences Division, **N. Agarwal** is Scientist, **A. Chakraborty** is Scientist, and **S. Mallick** is a graduate student, all at Space Applications Centre, Indian Space Research Organization (ISRO), Ahmedabad, India. **Jared Buckley** is a graduate student at the University of Massachusetts Dartmouth, North Dartmouth, MA, USA. **V. Shesu** is Scientist, Indian National Centre for Ocean Information Services, Hyderabad, India. **Amit Tandon** is Professor of Mechanical Engineering, University of Massachusetts Dartmouth, North Dartmouth, MA, USA.

ARTICLE CITATION

Sharma, R., N. Agarwal, A. Chakraborty, S. Mallick, J. Buckley, V. Shesu, and A. Tandon. 2016. Large-scale air-sea coupling processes in the Bay of Bengal using space-borne observations. *Oceanography* 29(2):192–201, http://dx.doi.org/10.5670/oceanog.2016.51.